

NONLINEAR ACOUSTOELECTRIC EFFECT AND AMPLIFICATION OF ULTRASOUND IN INDIUM ANTIMONIDE

P. E. ZIL'BERMAN, S. N. IVANOV, I. M. KOTELYANSKIĬ, G. D. MANSFEL'D and E. N. KHAZANOV

Institute of Radio Engineering and Electronics, USSR Academy of Sciences

Submitted June 15, 1972

Zh. Eksp. Teor. Fiz. 63, 1745-1751 (November, 1972)

The nonlinear acoustoelectric effect in crystals of finite length is calculated at high sound frequencies (when the sound wavelength is shorter than the carrier mean free path). Electronic amplification of sound and the acoustoelectric effect are investigated experimentally in indium antimonide crystals at 78° K for sound intensities 10<sup>-4</sup>-1 W/cm<sup>2</sup> and frequencies 1-2.3 GHz. The critical power characterizing the onset of nonlinearity and the "escape" component of the electron momentum relaxation time are calculated.

In pure n-InSb crystals at 78° K for frequencies above 1 GHz a collisionless mechanism plays the principal role in the electronic amplification of sound (Landau amplification of sound waves).<sup>[1]</sup> This means that at such frequencies the inequality  $ql > 1$  is satisfied, where  $q$  is the wave number of sound and  $l$  is the electron mean free path.<sup>[2,3]</sup>

As the sound intensity increases the Landau amplification effect begins to depend on the intensity. This nonlinear effect results when sound destroys the equilibrium distribution of electron momenta, after which the non-equilibrium electrons are involved in the amplification of the sound. Acoustoelectric nonlinearity of this type has been analyzed by one of the present authors for broad-spectrum sound beams,<sup>[4]</sup> and by others for monochromatic sound.<sup>[5,6]</sup> An important feature of this nonlinearity is that it appears at relatively low sound intensities ( $\sim 3 \times 10^{-2}$  W/cm<sup>2</sup> in n-InSb at 78° K). At sound intensities of this order in n-InSb the nonlinear limitation of amplification has been observed experimentally in<sup>[7]</sup>, where the experimental results agree qualitatively with the theory in<sup>[5,6]</sup>.

It has been shown<sup>[6]</sup> that the studied nonlinearity should be manifested in the acoustoelectric effect<sup>[1]</sup> as well as in sound amplification. In Sec. 1 of the present work, on the basis of previously derived formulas<sup>[6]</sup> for the gain and current density, the acoustoelectric effect in samples of finite length is calculated with account of the nonlinearity. A similar calculation for nonlinear amplification has been published in<sup>[9]</sup>. In Sec. 2 we present results obtained in an experimental investigation of both the acoustoelectric effect and the amplification of sound at different intensities.

1. CALCULATION OF THE ACOUSTOELECTRIC EFFECT

Let us consider the stationary propagation of sound in a crystal of finite length  $L$  under conditions that permit neglect of the reflected wave. The equation of continuity for a flux of sound energy  $W$  (watt/cm<sup>2</sup>) is

$$\frac{\partial W}{\partial x} + (\alpha + \alpha_L)W = 0, \tag{1}$$

where  $x$  is the coordinate along the sample, and  $\alpha$  and

<sup>1)</sup>We note that the nonlinear acoustoelectric effect at low frequencies ( $ql \ll 1$ ) has been studied by Proklov et al. [8].

$\alpha_L$  are the electronic and lattice coefficients of sound absorption. Assuming that the relaxation time  $\tau_p$  of electron momentum and the "escape" component  $\tau_0$  of the momentum relaxation time are independent of the energy, we obtain on the basis of<sup>[6]</sup>

$$\alpha = \alpha_0 \frac{1 - \mu E/v_s}{(1 + W/W_c)^{1/2}}, \quad j = en\mu E + \frac{\mu \alpha W}{v_s}. \tag{2}$$

Here  $\alpha_0$  is the linear electronic coefficient of sound absorption,  $j$  is the electron current density,  $n$  and  $\mu$  are the electron concentration and mobility, and  $v_s$  is the velocity of sound.

Equation (2) holds true when<sup>[6]</sup>

$$\hbar q^2 \tau_0 / m \gg 1, \tag{3}$$

where  $m$  is the effective electron mass. The electric field  $E(x)$  satisfies the relation

$$\int_0^L E(x) dx = V, \tag{4}$$

where  $V$  is the potential difference between the ends of the sample. The parameter  $W_c$  signifies the sound flux at the onset of nonlinearity. According to<sup>[9]</sup> we have

$$W_c = \frac{e^2 \rho v_s^3 q^2 \hbar^2 (1 + q^2 r_D^2)^2}{2(4\pi\beta e\tau_0)^2 q^4 r_D^4}, \tag{5}$$

where  $\rho$  and  $\epsilon$  are the density and dielectric constant of the crystal,  $r_D$  is the Debye screening radius, and  $\beta$  is the piezoelectric modulus. The inclusion of  $\tau_0$  in the expression (5) for  $W_c$  is associated physically with the fact that sound destroys the equilibrium distribution of the electrons only in a small region of momentum space near the planes  $p_x = mv_x \pm \hbar q/2$ . The relaxation of such localized (in  $p$  space) disturbances takes place within a time  $\tau_0$  (not  $\tau_p$ ). The relation between  $\tau_0$  and  $\tau_p$  has been analyzed by one of the present authors.<sup>[10]</sup>

Equations (1), (2), and (4) can be used to calculate the amplification and the acoustoelectric effect. Because of sound amplification the quantities  $W$ ,  $E$ , and  $n$  depend, in principle, on the  $x$ -coordinate. However, the concentration  $n$  can be considered to be practically constant, because the condition  $\alpha r_D \ll 1$  is always well satisfied. The part of the field  $E$  that is dependent on  $x$  contributes to the investigated acoustoelectric effect. However, in solving (1) we may neglect the acoustoelectric effect and replace  $E$  with the mean field  $V/L$ . In this way the growth of the sound flux  $W(x)$  is studied independently

of the acoustoelectric effect. The condition for the permissibility of this approach is

$$\delta = \frac{\mu W_c \alpha}{en v_s^2 (1 + \mu V / v_s L)} \ll 1. \quad (6)$$

In n-InSb we have  $\delta \sim 10^{-2}$ .

The flux  $W(x)$  obtained by solving (1) in zeroth order with respect to  $\delta$  is inserted into the equation (2) for the current  $j$ , which we then integrate over the length of the crystal. From (4) and the fact that  $j$  is independent of  $x$  we obtain the volt-ampere characteristic  $j(V)$ , which takes the acoustoelectric effect into account (in first order with respect to  $\delta$ ). At a given voltage  $V$  the acoustoelectric addition to the current is found to be

$$j_{ae} = \frac{\mu \gamma W_c}{v_s L} [\Phi_\gamma(w_{out}) - \Phi_\gamma(w_{in})], \quad (7)$$

where

$$\gamma = \frac{\alpha_o}{\alpha_L} \left( \frac{\mu V}{v_s L} - 1 \right),$$

$$\Phi_\gamma(w) = 2[(1+w)^{\gamma/2} + \gamma \ln |(1+w)^{\gamma/2} - \gamma|].$$

In the parameters  $w_{out} = W_{out}/W_c$  and  $w_{in} = W_{in}/W_c$ , the terms  $W_{in}$  and  $W_{out}$  are the input and output sound fluxes of the crystal. The relation between  $w_{out}$  and  $w_{in}$  is described by

$$-\alpha_L L = F_\gamma(w_{out}) - F_\gamma(w_{in}), \quad (8)$$

$$F_\gamma(w) = \frac{2\gamma^2}{\gamma^2 - 1} \ln |(1+w)^{\gamma/2} - \gamma| + \frac{1}{1+\gamma} \ln |(1+w)^{\gamma/2} + 1| - \frac{1}{\gamma - 1} \ln |(1+w)^{\gamma/2} - 1|.$$

When  $\alpha_L$  is known these expressions can be used to calculate the gain in the case of nonlinear electronic amplification. If nonlinear effects play no role ( $w_{out} \ll 1$ ), then from (6) and (7) we obtain

$$j_{ae} = \frac{\mu \alpha_o W_{in} (\mu V / v_s L - 1) \{1 - \exp[\alpha_o (\mu V / v_s L - 1) - \alpha_L] L\}}{v_s [\alpha_o (\mu V / v_s L - 1) - \alpha_L] L}. \quad (9)$$

In the other limiting case, where nonlinear effects do limit the amplification and a stationary wave propagates in the crystal, we obtain

$$j_{ae} = -\mu \alpha_L W_{st} / v_s, \quad (10)$$

where  $W_{st} = W_c (\gamma^2 - 1)$  is the sound flux in the stationary wave. In all intermediate cases (7) and (8) can be analyzed numerically.

At a given current  $j$  the acoustoelectric addition to the voltage is given by

$$V_{ae} = -\frac{\gamma W_c}{en v_s} [\Phi_\gamma(w_{out}) - \Phi_\gamma(w_{in})], \quad (11)$$

$$\gamma = \frac{\alpha_o}{\alpha_L} \left( \frac{j}{nev_s} - 1 \right).$$

As previously,  $w_{out}$  and  $w_{in}$  are related through Eq. (8). If given values of  $j$  and  $V$  are related through the equation  $j = en \mu (V/L)$ , then from (7) and (11) we derive the acoustoelectric addition

$$j_{ae} = -en \mu (V_{ae}/L). \quad (12)$$

This equation specifically relates the current through a short-circuited sample to the open-circuit voltage.

## 2. EXPERIMENT

The nonlinear acoustoelectric interaction was investigated in indium antimonide crystals with  $n = (2-4) \times 10^{14} \text{ cm}^{-3}$  and  $\mu = (6-7) \times 10^5 \text{ cm}^2/\text{V-sec}$  at  $78^\circ \text{ K}$ .

Piezoactive shear sound waves were excited in the [110] direction at 1–2.3 GHz. Sound was excited and registered with acoustoelectric transducers consisting of CdS films that had been grown on the end surfaces of the samples using the gas-transport reaction method. The loss at a single conversion in these epitaxial transducers amounted to 20–25 dB within the entire investigated frequency range. The sound input power was varied from  $10^{-4}$  to  $1 \text{ watt/cm}^2$ . We used the well-known echo method of registering signal pulses.

When an external electric field pulse was applied in order to induce electron drift in the direction of sound wave propagation, amplification of the sound was observed. The gain  $G$  over the length  $L$  of the active crystal region was

$$G = - \int_0^L \alpha dx.$$

In our experiments we measured the quantity

$$\int_0^L \alpha dx - \int_0^L \alpha_0 dx.$$

Because of the existing condition  $|\alpha| \gg |\alpha_0|$ , the measured quantity can be identified with the gain.

For the purpose of comparing the experimental results with the theory in Sec. 1 it was necessary to know the value of the lattice absorption coefficient  $\alpha_L$ , which was measured in independent experiments. The accuracy of the  $\alpha_L$  and  $G$  measurements was not worse than 10%. The velocity  $v_d$  was determined from the equation  $v_d = I/neS$ . Here  $I$  is the total current through the sample, and  $S$  is the cross-sectional area of the sample. The acoustoelectric current  $I_{ae}$  was observed in the form of a pulse on the top of the drift current pulse. When  $v_d > v_s$  the direction of  $I_{ae}$  became the opposite of the drift current direction.

The curves in Fig. 1 show how the electronic amplification depended on the sound input intensity  $W_{in}$  at different frequencies and a fixed value of the drift velocity. At  $W_{in} = (10^{-3}-10^{-2}) \text{ watt/cm}^2$  the gain begins to depend on the sound intensity. The frequency dependence is attributed to decreasing screening of the piezoelectric field of the wave as the frequency is increased.

Figure 2 shows how the electronic amplification (gain) depends on the drift at different values of  $W_{in}$ . As  $W_{in}$  is increased the gain diminishes by a factor of tens. The uppermost curve was plotted for the lowest sound input power and represents the linear case in the theory of the amplification. The bending of the curves at high

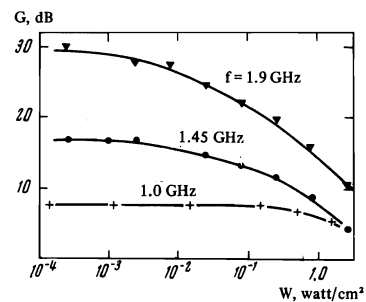


FIG. 1. Electronic amplification of sound in a crystal versus sound input power at different frequencies and a fixed drift velocity ( $v_d/v_s = 30$ ). The sample had concentration  $n = 4 \times 10^{14} \text{ cm}^{-3}$ ; the solid theoretical curves represent Eq. (8).

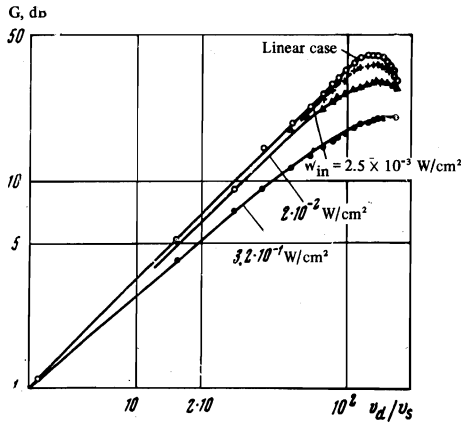


FIG. 2. Electronic amplification (gain) vs electron drift velocity at different sound input power levels, in crystal No. 16-c with  $n = 1.9 \times 10^{14} \text{ cm}^{-3}$ .

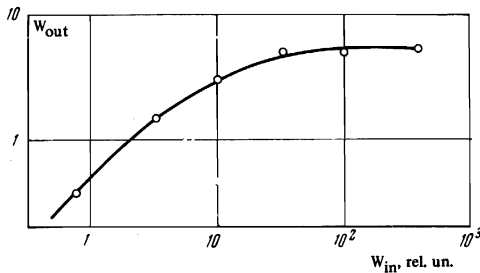


FIG. 3. Sound output power in the case of nonlinear amplification vs input power at  $f = 2.3 \text{ GHz}$  in a crystal with  $n = 4 \times 10^{14} \text{ cm}^{-3}$ .

drift velocities resulted from heating of the electron gas.

It has been shown in<sup>[7]</sup> that the reduction of the electronic amplification as the sound intensity increases can, in principle, lead to the creation of a stationary sound wave. The sound output can then remain constant over a fairly broad range of the input power (depending on the length of the crystal). The saturation, shown in Fig. 3, of the dependence of the normalized output power on the input power provides evidence of the establishment of a stationary wave regime in the exit section of the crystal.

Acoustoelectric nonlinearity at  $ql > 1$  is also manifested very clearly in the acoustoelectric current, the dependence of which on the power for different values of  $v_d/v_s$  is shown in Fig. 4. Instead of the linear dependence of  $I_{ae}(W_{in})$  predicted by the linear theory, the observations approximate  $I_{ae} \sim W_{in}^{1/2}$ .

Figure 5 shows a family of curves representing the dependence of  $I_{ae}$  on  $v_d/v_c$  at different values of  $W_{in}$ . The measured currents are lower than the predictions of the linear theory (by a factor of about 100 in the case of the highest  $W_{in}$ ).

The solid theoretical curves in Figs. 1, 4, and 5 represent equations of the preceding section. We combine the data on the gain and the acoustoelectric current; the gain curves yield the value of  $W_{in}/W_c$ , which is then used to determine  $W_c$  from the current curves in Figs. 4 and 5. This is possible because the equation for  $I_{ae}$  contains  $W_c$  as well as the ratio  $W_{in}/W_c$ . In Figs. 4 and 5 the best agreement between theory and experiment is found for the threshold power  $W_c = 2$

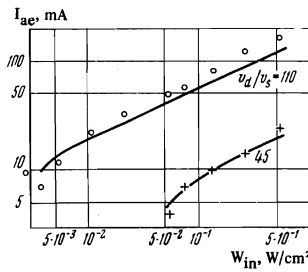


FIG. 4

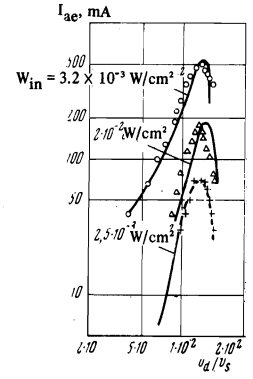


FIG. 5

FIG. 4. Acoustoelectric current versus sound input power flux at a fixed drift velocity and frequency  $f = 1.87 \text{ GHz}$  in crystal sample No. 14-b with  $n = 1.8 \times 10^{14}$ . The solid curves were calculated on the basis of Eq. (7).

FIG. 5. Acoustoelectric current versus electron drift velocity at  $f = 1.87 \text{ GHz}$  and different sound input power levels in crystal No. 16-c with  $n = 1.9 \times 10^{14} \text{ cm}^{-3}$ . The solid curves were calculated on the basis of Eq. (7).

$\times 10^{-1} \text{ watt/cm}^2$ . With  $W_c$  known, Eq. (5) is used to calculate and compare  $\tau_0$  with  $\tau_p$ , which is determined from the measured mobility  $\mu = e\tau_p/m$ . We thus obtain

$$\tau_0 / \tau_p \approx 0.3. \tag{13}$$

We note that  $W_c$  and  $\tau_0$  were obtained without using the measured values of  $W_{in}$ , thus excluding considerable error that is associated with the measurement of  $W_{in}$ . We estimated that the remaining errors incurred in determining  $\tau_0$  cannot increase the ratio given in (13) by more than 80%.

Thus the parameter  $W_c$  can be adjusted to obtain satisfactory agreement between the experimental and theoretical dependences of the gain  $G$  and current  $I_{ae}$  on  $W_{in}$  and on the drift velocity  $v_d$ . The relaxation time  $\tau_0$  that would correspond to the selected value of  $W_c$  according to (5) is smaller than the value of  $\tau_p$  [see (13)]; this is consistent with the theoretical concepts. Indeed, according to the theory  $\tau_0$  is the ‘escape’ (component of the) momentum relaxation time and, by definition, cannot exceed  $\tau_p$ . However, from the value of  $\tau_0$  according to (13) it follows that the condition (3) for the applicability of the theory may possibly not be fulfilled in the given experimental situation. It is therefore of interest to compare experiment with the theory presented in<sup>[5]</sup>, which was developed for the case in which the inequality (3) is reversed. To permit this comparison the theory of<sup>[5]</sup> must be developed further, particularly for the purpose of deriving formulas integrated over the length of the crystal.

Further experimental and theoretical study of nonlinear Landau damping (and amplification) of sound waves can yield information about the ‘escape’ momentum relaxation time  $\tau_0$ , which is important because it describes the relaxation of ‘local’ (in momentum space) disturbances of the equilibrium electron distribution. Such ‘local’ perturbations can arise not only through the interaction of electrons with high-frequency sound, but also in certain other cases such as electron beams in solids, the ‘needle-shaped’ distribution of electrons in a high electric field etc.

The authors wish to thank Yu. V. Gulyaev and S. G. Kalashnikov for an interesting discussion of this work.

<sup>1</sup>R. K. Route and G. S. Kino, *Appl. Phys. Lett.* **14**, 97 (1969); E. Voges, *Solid State Commun.* **8**, 1733 (1970).

<sup>2</sup>L. É. Gurevich, *Izv. Akad. Nauk SSSR, ser. fiz.* **21**, 112 (1957) [*Bull. Acad. Sci. USSR, Phys. Ser.* **21**, 106 (1957)].

<sup>3</sup>A. I. Akhiezer, M. I. Kaganov, and G. Ya. Lyubarskiĭ, *Zh. Eksp. Teor. Fiz.* **32**, 837 (1957) [*Sov. Phys.-JETP* **5**, 685 (1957)].

<sup>4</sup>P. E. Zil'berman, *Fiz. Tverd. Tela* **12**, 1014 (1970) [*Sov. Phys.-Solid State* **12**, 796 (1970)].

<sup>5</sup>Yu. M. Gal'perin and V. D. Kagan, *Zh. Eksp. Teor. Fiz.* **59**, 1657 (1970) [*Sov. Phys.-JETP* **32**, 903 (1971)]; Yu. M. Gal'perin, V. D. Kagan, and V. I. Kozub, *Zh.*

*Eksp. Teor. Fiz.* **62**, 1521 (1972) [*Sov. Phys.-JETP* **35**, 798 (1972)].

<sup>6</sup>P. E. Zil'berman, *Zh. Eksp. Teor. Fiz.* **60**, 1943 (1971) [*Sov. Phys.-JETP* **33**, 1048 (1971)].

<sup>7</sup>S. N. Ivanov, I. M. Kotelyanskiĭ, G. D. Mansfel'd, and E. N. Khazanov, *ZhETF Pis. Red.* **13**, 283 (1971) [*JETP Lett.* **13**, 201 (1971)].

<sup>8</sup>V. V. Proklov, Yu. V. Gulyaev, and A. I. Morozov, *Fiz. Tverd. Tela* **14**, 968 (1972) [*Sov. Phys.-Solid State* **14**, 832 (1972)].

<sup>9</sup>P. E. Zil'berman, *Fiz. Tekh. Poluprov.* **5**, 1240 (1971) [*Sov. Phys.-Semicond.* **5**, 1092 (1972)].

<sup>10</sup>P. E. Zil'berman, *Fiz. Tverd. Tela* **10**, 2088 (1968) [*Sov. Phys.-Solid State* **10**, 1635 (1969)].

Translated by I. Emin

193